



Proton conductive properties of composite membranes containing uniaxially aligned ultrafine electrospun polyimide nanofiber

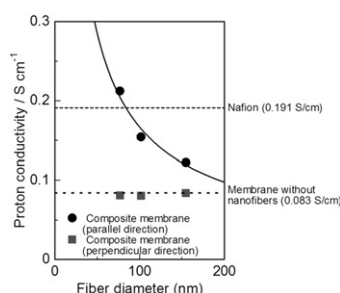
Takuya Tamura, Ryouhei Takemori, Hiroyoshi Kawakami*

Department of Applied Chemistry, Tokyo Metropolitan University, Hachioji, Tokyo 192-0397, Japan

HIGHLIGHTS

- ▶ We fabricated novel uniaxially aligned ultrafine copolyimide nanofibers.
- ▶ We prepared novel composite membranes containing the nanofibers.
- ▶ The parallel proton conductivity increased with the decreasing nanofiber.
- ▶ The parallel conductivity was higher than the perpendicular conductivity.

GRAPHICAL ABSTRACT



ARTICLE INFO

Article history:

Received 7 March 2012

Received in revised form

16 May 2012

Accepted 31 May 2012

Available online 12 June 2012

Keywords:

Five-membered ring sulfonated polyimide

Aligned ultrafine polyimide nanofiber

Electrospinning

Proton conductivity

Composite membrane

ABSTRACT

The nanofiber electrospun from the five-membered ring sulfonated polyimide containing the fluorinated group showed an ultrafine and uniform non-beaded structure and the optimized electrospinning conditions produced the sulfonated polyimide nanofibers with several appropriate diameters ranging from 80 to 160 nm. Novel sulfonated copolyimide membranes containing uniaxially aligned ultrafine sulfonated copolyimide nanofibers were prepared for proton exchange membrane fuel cell applications. The proton conductivity of the composite membrane in the parallel direction to the nanofibers alignment increased with the decreasing nanofiber diameter and the increasing amount of nanofibers in the composite membrane and reached 0.3 S cm^{-1} at 90°C and 98% RH. In addition, the parallel proton conductivity indicated significantly higher values when compared to that determined for the composite membrane in the perpendicular direction or for the membrane without nanofibers prepared by a conventional solution-casting method. The composite membranes also showed higher chemical stabilities than those of the membrane without nanofibers. Consequently, nanofibers proved to be promising proton exchange materials and the composite membranes containing nanofibers may have potential application for use in fuel cells.

© 2012 Elsevier B.V. All rights reserved.

1. Introduction

Proton exchange membrane fuel cells, which efficiently convert chemical energy into electrical energy via oxidation and reduction reactions, are receiving considerable attention as an alternative

energy source because of their high energy efficiency and no emissions of pollutants [1]. One of the most important technical focuses on developing proton exchange membranes that are able to achieve a high proton conductivity, low gas permeability of the fuel and oxidant, and sufficient chemical stabilities [2,3]. At present, the perfluorosulfonated aliphatic polymer membranes, such as Nafion®, have been widely used because of their excellent chemical stability as well as high-proton conductivity [4,5]. However, they have several drawbacks including high cost, low thermal stability,

* Corresponding author. Tel.: +81 426 77 1111x4972; fax: +81 426 77 2821.

E-mail address: kawakami-hiroyoshi@tmu.ac.jp (H. Kawakami).

and high gas permeability. Recently, much effort has been directed to the development of novel polymer electrolyte membranes based on sulfonated aromatic hydrocarbon polymers, which have been widely synthesized as alternate candidates due to their excellent chemical and thermal stabilities and good mechanical strength [6–14]. Although the proton conductivity of the membranes is well-known to increase with the increasing concentration of sulfonic acid groups, the high concentration of sulfonic acid groups results in an unfavorable swelling of the membranes and a dramatic loss in their mechanical properties [15,16]. Therefore, one of the important objectives for designing the polymer electrolyte membranes is the development of new polymer membranes combining a high proton conductivity and good membrane stabilities.

Electrospinning provides a simple and versatile method for the generation of ultrathin fibers from a rich variety of materials that include polymers, ceramics, and their composites [17–23]. Recently, electrospun fibers have attracted significant attention due to their potential applications in conductive fibers, filtration membranes, water purification, and tissue engineering scaffolds. In addition, electrospinning is capable of producing fibers with diameters in the nanometer range. Many synthetic and natural polymers have been electrospun to form nanofibers with a small diameter. The electrospun fibrous mats offer a great advantage in terms of the recovery and easy handling of the materials. However, there are only a few reports in the literature on the proton conductivity of electrospun nanofibrous mats, in addition, the fibrous structure was an isotropic non woven mat [24–27]. We have prepared polymer electrolyte membranes composed of aligned nanofibers with ca. 200 nm diameters for the first time, and revealed that the composite membranes showed a higher proton conductivity and lower gas permeability than the membrane without nanofibers [28]. In addition, we calculated the apparent proton conductivity of a single nanofiber using a simulation equation, and the apparent proton conductivity significantly increased when compared to the composite membrane containing the nanofibers and was approximately twenty times higher than that of the composite membrane. The sulfonated six-membered ring (naphthalenic) polyimide synthesized in a previous study has been proposed to be a promising material for use as a proton exchange membrane, because the polyimide exhibited excellent chemical and thermal stabilities [29,30]. However, it is very difficult to prepare the ultrafine and uniform non-beaded nanofibers using the electrospinning method from the six-membered ring polyimide solution, because the solubility of the polyimide for organic solvents is not enough. That is, the preparation of the polyimide nanofibers electrospun from the six-membered ring polyimides has a limitation.

On the other hand, the five-membered ring polyimides exhibit low chemical and thermal stabilities compared to those of the six-membered ring polyimides, however, the former polyimides generally have a better solubility in organic solvents compared to the latter polyimides. In particular, the five-membered ring polyimides containing the fluorinated group indicate an excellent solubility. We have already demonstrated that the nanofiber electrospun from the five-membered ring polyimides containing the fluorinated group can easily form an ultrathin and uniform non-beaded structure [22,23]. We now describe the preparation of novel composite membranes composed of uniaxially aligned ultrathin nanofibers electrospun from a novel fluorinated five-membered ring copolyimide bearing sulfonic acid groups. In particular, we focused on the effects of the nanofiber diameters on the proton conductivity of the composite membrane. The proton conductivities and other properties of the composite membranes were discussed for future applications in a fuel cell.

2. Experimental

2.1. Materials

2,2'-Bis(3,4-dicarboxyphenyl)hexafluoropropane dianhydride (6FDA) was purchased from the Central Glass Co. (Saitama, Japan) and was purified by sublimation before use. 4,4'-Diaminobiphenyl-2,2'-disulfonic acid (BDSA) was purchased from the TokyoKasei Co. (Tokyo, Japan) and was purified by dissolution in a triethylamine aqueous solution and then precipitated in 1 N H₂SO₄. Finally, the BDSA was dried in a vacuum oven at 70 °C for 12 h. 2,2-Bis[4-(4-aminophenoxy)phenyl]-hexafluoropropane (APPF) was purchased from Wako Chemical Ind. (Osaka, Japan) and was recrystallized twice from an ethanol solution prior to use. Nafion® 117 was used in this study as the control membrane. The membranes were obtained from the DuPont Co. (Tokyo, Japan). All other reagents were purchased from Kanto Chemical (Tokyo, Japan) and were used as received.

2.2. Syntheses of sulfonated polyimides

The sulfonated copolyimide, 6FDA-BDSA-*r*-APPF (Fig. 1), was synthesized as follows: In a three-neck round bottom flask, APPF (1.56 g, 3.00 mmol) and BDSA (2.41 g, 7.00 mmol) were dissolved in *m*-cresol (30 ml) in the presence of triethylamine (TEA, 6.0 ml) at 80 °C for 4 h, and 6FDA (4.44 g, 10.0 mmol) was then added to the solution. After stirring the solution at 120 °C for 24 h, benzoic acid (1.37 g, 11.2 mmol) and triethylamine (TEA, 3.0 ml) were added, then stirred 180 °C for 24 h. The molar ratio of BDSA to APPF was set at 7:3. The 6FDA-BDSA-*r*-APPF (TEA form) was precipitated into ethyl acetate, washed several times with fresh ethyl acetate, and dried under vacuum at 150 °C for 12 h. The molecular weights (M_w and M_n) of the sulfonated copolyimide were determined by gel-permeation chromatography (detector: Jasco 830-R1 monitor) using two Shodex SB-806 HQ and SB-804 HQ columns. Dimethylformamide containing 0.01 M lithium bromide was used as the eluent at a flow rate of 1.0 ml min⁻¹. The molecular weights were estimated by comparing the retention times on the columns to those of standard polystyrene.

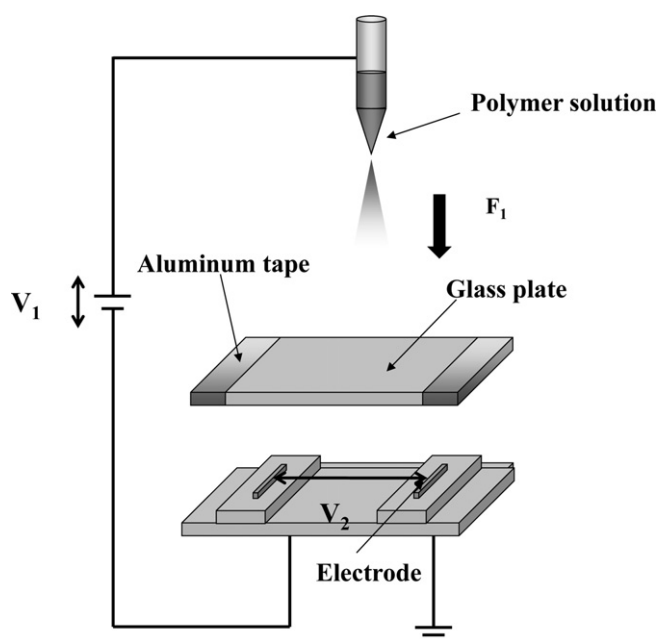


Fig. 1. Diagram of the electrospinning method.

2.3. Preparation of composite membranes containing aligned electrospun sulfonated copolyimide nanofibers

The experimental set-up used for the preparation of the aligned sulfonated copolyimide nanofibers is shown in Fig. 1 [22]. The nanofibers were fabricated using an electrospinning apparatus (Fuence, Co., Ltd., ES-1000, Tokyo, Japan). A collector was simply fabricated using two conductive aluminum foils and a glass plate insulator. The collector could be removed from the apparatus. The sizes of the aluminum foil and the glass plate were $1 \times 7 \text{ cm}^2$ and $10 \times 7 \text{ cm}^2$, respectively. The width of the gap between the two aluminum plates was 3 cm. 6FDA-BDSA-*r*-APPF (Tea form) was dissolved in DMF at a concentration of 12 wt%, 15 wt%, or 18 wt%. The viscosity of the polyimide solution was measured with a viscometer (Toki Sangyo Co., Ltd., RE-85, Tokyo, Japan). The viscosity at a 12 wt% polyimide solution was 1160 mPa s, and the viscosity increased with the increasing concentration. The electrospinning parameters were as follows: the polymer solution was loaded into a 1-ml syringe as the spinneret. A syringe pump was used to squeeze out the polymer solution at a constant speed through a needle with an inner diameter of 0.21 mm. V_1 is the applied voltage between the syringe and the collector, and V_2 is the applied voltage between the two aluminum plates as the electrodes. Uniaxially aligned nanofibers were deposited on the filter paper as the support medium of the nanofibers, located on the collector by the electrospinning method. The thickness and amount of the uniaxially aligned nanofibrous membrane were controlled by the electrospinning deposition time. To remove the residual solvent from the fabricated nanofibers, vacuum drying was carried out at 150 °C for 10 h. The 6FDA-BDSA-*r*-APPF nanofibers were then acidified with a 0.1 M HCl solution for 24 h to obtain the 6FDA-BDSA-*r*-APPF nanofibers (proton form), and were dried under vacuum at 80 °C for 12 h. The nanofibers were observed using a scanning electron microscope (SEM, JXP-6100P, JEOL, Tokyo, Japan). To determine the diameter, the electrospun nanofibers ($2 \times 2 \text{ cm}^2$) were fixed on a flat sample folder, then coated with gold for 120 s at a current of 10 mA under a vacuum of 10 Pa. At least five pictures and 25 nanofibers were used to determine each diameter.

In a vessel, the appropriate amount of the same sulfonated polyimide, 6FDA-BDSA-*r*-APPF (TEA form), was dissolved in DMSO. The solution was poured on the aligned 6FDA-BDSA-*r*-APPF (proton form) nanofibers in a petri dish, and the mixture solution was dried in a vacuum oven at 110 °C for 12 h. After drying, the composite membrane containing the aligned 6FDA-BDSA-*r*-APPF nanofibers was acidified with a 0.1 M HCl solution for 24 h, then finally washed with deionized water. The resulting membrane was dried in a vacuum oven at 80 °C for 24 h. The thickness of the membrane was approximately 30 μm .

2.4. Characterization of the composite membranes

The ion exchange capacity (IEC) of the composite membrane was measured by classical titration using NaCl and NaOH solutions [8,11]. The water uptake of the composite membrane containing the nanofibers was gravimetrically measured from the dried and humidified membranes [8,11]. The membranes were dried in a vacuum oven at 80 °C for 10 h and then immersed in liquid water at room temperature. After 24 h, the membrane was then wiped dry and quickly weighed. The water uptake was calculated using Eq. (1)

$$W(\%) = \frac{W_s - W_d}{W_d} \times 100 \quad (1)$$

where W_s and W_d are the weights of the wet and dry membranes, respectively.

Low-temperature DSC experiments were performed using a Shimadzu DSC-60 (Tokyo, Japan). Fully-hydrated membrane samples were carefully blotted to remove any surface water and then immediately transferred to sealed aluminum pans. The samples were quickly placed in the calorimeter and cooled to $-50 \text{ }^\circ\text{C}$. The samples were then heated to $20 \text{ }^\circ\text{C}$ at the rate of $5 \text{ }^\circ\text{C min}^{-1}$. The thermal behavior of the composite membrane was evaluated by a thermogravimetric analysis (TGA: Seiko TG/DTA60/60H, Tokyo, Japan) from room temperature to $600 \text{ }^\circ\text{C}$ at the heating rate of $10 \text{ }^\circ\text{C min}^{-1}$ in a nitrogen atmosphere.

The stability of the composite membranes containing the nanofibers to oxidation was investigated by immersing the membranes ($1 \text{ cm} \times 1 \text{ cm}$) in Fenton's reagent (2 ppm FeSO_4 in 3% H_2O_2) at $80 \text{ }^\circ\text{C}$. The hydrolytic stability of the membranes ($1 \text{ cm} \times 1 \text{ cm}$) was performed by immersing them in deionized water at $80 \text{ }^\circ\text{C}$. The stabilities were characterized by the time it took the membrane to completely dissolve.

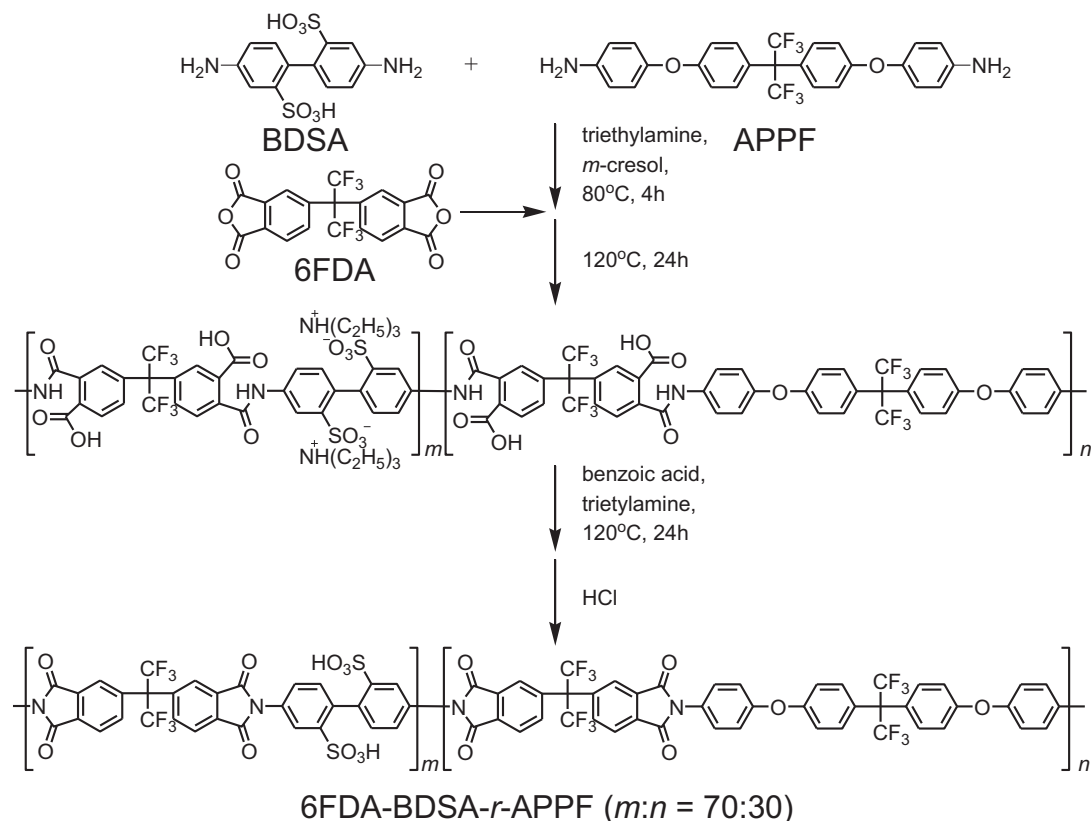
The proton conductivity was measured by electrochemical impedance spectroscopy over the frequency range from 50 Hz to 500 kHz (Hioki 3532-50, Tokyo, Japan) as reported in previous papers [8,11]. The membranes ($1.0 \times 3.0 \text{ cm}^2$) and two blackened platinum plate electrodes were placed in a Teflon cell to measure the proton conductivities in the parallel and perpendicular directions to the aligned nanofiber direction. The distance between the two electrodes was 1.0 cm. The cell was placed in a thermo-controlled humidity chamber to measure the temperature and relative humidity dependence of the proton conductivity.

3. Results and discussion

3.1. Preparation of the uniaxially aligned ultrafine sulfonated copolyimide nanofibers

Scheme 1 shows the synthetic procedure for the sulfonated copolyimide (6FDA-BDSA-*r*-APPF), which was obtained by thermal imidation of the precursor poly(amic acid) in the presence of benzoic acid and triethylamine. The $^1\text{H-NMR}$ spectrum of the obtained sulfonated copolyimides indicated the successful synthesis of the objective copolyimide in the TEA form. The obtained 6FDA-BDSA-*r*-APPF was soluble in DMF, DMAc, DMSO, and *N*-methylpyrrolidone (NMP), and showed a high molecular weight with a narrow polydispersity ($M_w = 3.4 \times 10^5$, $M_w/M_n = 1.8$).

The electrospinning process is a method of discharging a polymer solution in air from a nozzle under high voltage and producing a nanofiber by exploiting the electrostatic repulsion of the polymer solution (Fig. 1). It has been reported that the shape of the initiating droplet through the spinneret can be changed by the electrospinning conditions, such as the applied voltage, viscosity and feeding rate of the polymer solution, the distance between the spinneret and the grounded plate collector, and the relative humidity (RH) of the apparatus. In particular, significant morphological changes were found when the concentration or viscosity of the polymer solution was changed, which means that the concentration or viscosity of the polymer solution is one of the most effective variables to control the nanofiber morphology. We found that it is impossible to fabricate a continuous nanofiber at a concentration of 6FDA-BDSA-*r*-APPF dissolved in DMF below 12 wt%. It was found that the nanofibers electrospun at concentrations below 12 wt% were composed of a mixture of fibers and beads. The electrospinning conditions except for the polymer concentrations were optimized and fixed as follows: The applied V_1 and V_2 voltages were 20 and 1 kV, respectively. The feeding rate of the polymer solution was 0.096 ml h^{-1} . The distance between the spinneret and the grounded plate was 10 cm. Fig. 2 shows SEM



Scheme 1. Synthesis of the sulfonated copolyimide (6FDA-BDSA-r-APPF).

images of the aligned electrospun 6FDA-BDSA-r-APPF nanofibers with the polymer concentrations of 12, 15, and 18 wt%. These images clearly demonstrated that the nanofibers were uniaxially aligned and were individually deposited across the gap between the aluminum plates without any aggregation. It is considered that the electrostatic forces formed between the charged nanofiber and the aluminum plate determined the alignment direction of the nanofibers. In addition, the nanofibers had a uniform fiber-diameter for each polymer concentration, and the mean diameters of the nanofibers at 12, 15, and 18 wt% polymer concentrations were 77 ± 11 , 102 ± 19 , and 157 ± 11 nm ($n = 25$), respectively. We succeeded in preparing g uniaxially aligned non-beaded nanofibers as compared to those fabricated from the six-membered ring polyimides reported in our previous reports [27] by using 6FDA-BDSA-r-APPF, which possesses more flexible structure and a good solubility for organic solvents. In addition, we also succeeded in preparing an ultrafine and uniform nanofiber with a diameter of less than 100 nm by using the 6FDA-BDSA-r-APPF, although the

nanofibers fabricated from the six-membered ring polyimides indicated a diameter of more than 200 nm [27].

3.2. Preparation and characterizations of the composite membranes containing aligned nanofibers

The composite membranes were prepared by pouring the DMSO solutions of 6FDA-BDSA-r-APPF (TEA form) onto the aligned 6FDA-BDSA-r-APPF (proton-form) nanofibers in a petri dish. The contents of the nanofibers in the composite membranes were controlled at 10, 20, or 30 wt%. The ion exchange capacities (IECs) of the composite membranes containing the 10 wt% nanofibers with various diameters were measured by a titration method (Table 1). All of the composite membranes had similar IECs regardless of their fiber diameters.

The water uptakes of the composite membranes are summarized in Table 1. The number of water molecules per sulfonic groups (λ) was calculated from the water uptake results using Eq. (2).

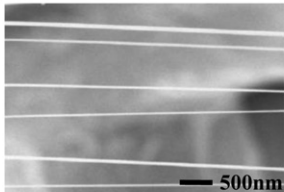
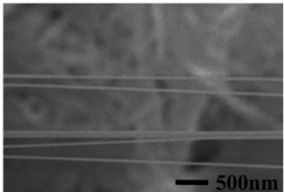
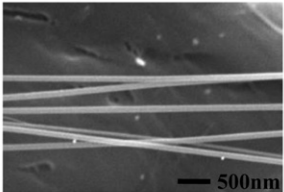
Polymer concentration	12wt%	15wt%	18wt%
SEM images			
Mean fiber diameter	77 ± 11 nm	102 ± 19 nm	157 ± 11 nm

Fig. 2. SEM images of the aligned electrospun nanofibers.

Table 1

Ion exchange capacity (IEC), water uptake, λ , λ_f , and λ_b of the membranes with and without nanofibers.

Membrane	IEC ^a (meq g ⁻¹)	Water uptake (%)	λ^b	λ_f^c	λ_b^d
Membrane without nanofibers	1.65	32	11	2	9
Composite membrane ^e (Fiber diameter: 77 nm)	1.63	38	13	1	12
Composite membrane ^e (Fiber diameter: 102 nm)	1.63	42	14	2	12
Composite membrane ^e (Fiber diameter: 157 nm)	1.65	42	14	3	11

^a Calculated by titration.

^b Number of water molecules per sulfonic groups.

^c Number of free water molecules per sulfonic group.

^d Number of bound waters per sulfonic group.

^e Containing 10 wt% aligned nanofibers.

$$\lambda = \frac{n(\text{H}_2\text{O})}{n(\text{SO}_3^-)} = \frac{\text{WS}}{18\text{IEC}} \quad (2)$$

where $n(\text{H}_2\text{O})$ is the H_2O molar number, $n(\text{SO}_3^-)$ is the SO_3 group's mole number, WS is the water uptake value by weight, IEC is the ion exchange capacity based on titration measurements, and 18 corresponds to water's molecular weight. It is noteworthy that the composite membranes had slightly higher water uptakes and λ values than the membrane without nanofibers. In order to understand the hydrated states of the membranes, endothermic peaks corresponding to the melting water were measured by DSC to give the number of free water molecules per sulfonic group (λ_f) [28]. The number of bound waters per sulfonic group (λ_b) was calculated from Eq (3).

$$\lambda = \lambda_f + \lambda_b \quad (3)$$

where λ is the total hydration number calculated from Eq (2). The number of total water molecules per sulfonic group was almost constant ($\lambda \sim 14$) in all the composite membranes. On the other hand, the fraction of the bound water slightly increased by decreasing the fiber diameter. This may suggest that the interaction among the polymer chains becomes stronger in the thinner nanofibers to bind more water molecules within the nanofibers.

The thermal stabilities of the composite membranes were investigated by thermogravimetric analysis (TGA) measurements. Fig. 3 shows the TGA curves of the composite membranes containing the aligned nanofibers with different fiber diameters. The curves of the composite membranes were similar to that measured in the sulfonated copolyimide membrane without nanofibers. The loss above 280 °C was due to the desulfonation from 6FDA-BDSA-r-APPF. The weight loss above 550 °C was ascribed to the decomposition of

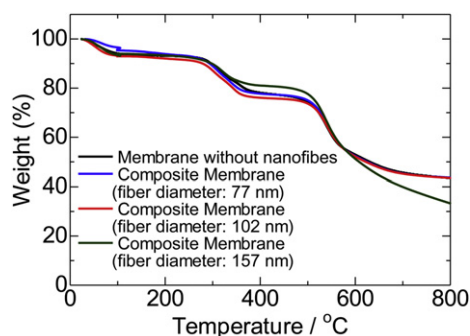


Fig. 3. Thermogravimetric analysis curves of the composite membranes and the membrane without nanofibers.

the polymer main chain. All of the membranes had a sufficient thermal stability to be used for fuel cell applications.

3.3. Proton conductivity of the composite membranes

The proton conductivities of the composite membranes were measured using electrochemical impedance spectroscopy in the parallel and perpendicular directions to the aligned nanofiber direction. $\sigma_{||}$ and σ_{\perp} denote the proton conductivities in the parallel and perpendicular directions to the aligned nanofiber direction, respectively. Table 2 shows the effect of the nanofiber diameter on the proton conductivity of the composite membranes. The proton conductivity of the 6FDA-BDSA-r-APPF membrane without nanofibers was ca. 0.08 S cm⁻¹ at 90 °C and 98% RH regardless of the measuring directions, indicating that the membrane had a homogeneous and isotropic morphology. On the other hand, the composite membranes showed different proton conductivities in the parallel and perpendicular directions, and the parallel proton conductivities were higher than the perpendicular ones for all the composite membranes. Since the parallel proton conductivities were higher than those of the 6FDA-BDSA-r-APPF membrane without nanofibers, such high conductivities of the composite membranes in parallel direction could originate from the aligned nanofibers. In addition, the composite membranes containing thinner nanofibers had higher parallel proton conductivities, and the values reached 0.212 S cm⁻¹ at 90 °C and 98% RH in the composite membrane containing nanofibers with 77-nm diameters. The increase in the parallel proton conductivities with the decreasing fiber diameters was apparent from Fig. 4 and the parallel proton conductivities depended on the diameter. In most of the polymer electrolyte membranes, the proton conductivities of the membranes are strongly related to the number of sulfonic acid groups or the water content of the membrane, thus the polymer electrolyte membranes absorbing a large amount of water typically have a high proton conductivity. Therefore, there is generally a good correlation between the proton conductivity and IEC or water uptake. However, as shown in Table 2, these values for the composite membranes and the membrane without nanofibers are almost constant, therefore, we postulate that ionic channels were formed in the nanofibers and that the protons were rapidly and efficiently transported in the nanofibers, especially, in the thinner nanofibers. On the other hand, the perpendicular proton

Table 2

Ion exchange capacity (IEC), parallel and perpendicular proton conductivities, and oxidative and hydrolysis stabilities of the membranes with and without nanofibers.

Membrane	IEC (meq g ⁻¹)	Proton conductivity		Oxidative stability ^c (h)	Hydrolysis stability ^d (h)
		$\sigma_{ }^a$ (S cm ⁻¹)	σ_{\perp}^b (S cm ⁻¹)		
Membrane without nanofibers	1.65	0.0836	0.0823	9	420
Composite membrane (Fiber diameter: 77 nm)	1.63	0.212	0.0805	12	750
Composite membrane (Fiber diameter: 102 nm)	1.63	0.154	0.0808	13	750
Composite membrane (Fiber diameter: 157 nm)	1.65	0.122	0.0837	13	750

^a Proton conductivity in parallel direction to fiber direction at 90 °C and 98% RH.

^b Proton conductivity in perpendicular direction to fiber direction at 90 °C and 98% RH.

^c The hydrolysis stability was measured by the time that the membranes dissolved in water at 80 °C.

^d The oxidative stability was measured by the time that the membranes completely dissolved in Fenton reagent at 80 °C.

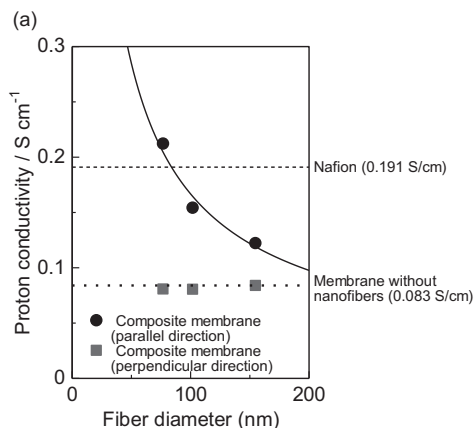


Fig. 4. Proton conductivities of the composite membrane containing 10 wt% nanofibers with various fiber diameters.

conductivities of the composite membranes were constant and did not depend on the diameter. In a previous study, the degree of orientation of the electrospun six-membered ring polyimide nanofibers was low, and the perpendicular proton conductivity in the composite membrane containing the nanofibers was significantly higher than that measured in the membrane without the nanofibers [28]. Based on the comparison between the two nanofibers, we concluded in this study that the high degree of orientation of the aligned nanofiber electrospun in the parallel direction induced the increase in only the parallel proton conductivity.

Fig. 5(a) shows the temperature dependence of the parallel proton conductivities of the composite membranes containing the nanofibers with 77-nm diameters at 98% relative humidity. In order to further investigate the effects of the aligned nanofibers on the proton conductivity, the composite membranes containing different nanofiber contents, 20 and 30 wt%, were also prepared and studied. It was found that the composite membranes showed higher proton conductivities when compared to the membrane without nanofibers at all temperatures. However, the proton conductivities of the composite membranes containing the higher nanofiber contents were slightly higher than that of the composite membrane with 10 wt% nanofibers.

The relative humidity dependence of the proton conductivity for the membranes at 90 °C is depicted in Fig. 5(b). The composite

membranes showed high proton conductivities comparable to that of Nafion at a high humidity and high temperature. At a lower humidity, however, the proton conductivity decreased to around 10^{-3} S cm $^{-1}$. This is the behavior often observed for the sulfonated aromatic hydrocarbon polymers. However, the composite membranes indicated higher values than the membrane without nanofibers at all humidities. Among the composite membranes, the proton conductivities of the composite membranes increased with the increasing nanofiber contents (maximum 0.302 S cm $^{-1}$ at 90 °C and 98% RH), and this tendency became pronounced at the lower relative humidities. At 30% RH, the conductivity of the composite membrane containing 30 wt% nanofibers with 77-nm diameters was one order higher than that of the membrane without nanofibers. This may be because the composite membrane has a high amount of bound water as shown in Table 1.

3.4. Membrane stabilities of the composite membranes

Generally, most of the membranes contain a high number of sulfonic acid groups to enhance the proton conductivity, but resulting in an unfavorable swelling of the membranes and a dramatic loss in their mechanical properties. Therefore, membrane stability plays a very important role in the properties of the proton exchange membranes. In this study, the oxidative and hydrolytic stabilities of the composite membranes were evaluated in Fenton's reagent and water at 80 °C, as shown in Table 2. The 6FDA-BDSA-r-APPF membrane without nanofibers had a relatively good resistance to the oxidation and hydrolytic degradations when compared to other sulfonated polyimide membranes [5–8]. For comparison between the composite membranes and the 6FDA-BDSA-r-APPF membrane without nanofibers, all of the composite membranes indicated longer times to be fully dissolved in Fenton's reagent or hot water. These findings suggest that the composite membranes containing the aligned nanofibers have a better stability toward the oxidation and hydrolytic degradations, although the chemical structures and the IEC values of the membranes were almost equal. We considered that the oriented and ordered molecular architecture in the nanofibers might have an influence on the membrane stabilities.

It was found that the proton conductivities and membrane stabilities of the composite membranes were superior to that in a membrane with no nanofibers. The composite membranes, however, were still not sufficient for use as practical materials in fuel cell electrolytes due to their insufficient stability and relatively low proton conductivity especially at low relative humidities. Therefore, future research will evaluate the above factors by determining the proton conductivities and stabilities of the nanofibers themselves.

4. Conclusions

The five-membered ring sulfonated copolyimide, 6FDA-BDSA-r-APPF, possessing a flexible polymer structure and good solubility for organic solvents produced uniform non-beaded sulfonated copolyimide nanofibers by an electrospinning method and ultrafine nanofibers down to 77-nm diameters. Novel composite membranes, which were composed of uniaxially aligned ultrafine sulfonated copolyimide nanofibers and sulfonated copolyimide, were prepared by the electrospinning and solution-casting methods. The composite membrane containing nanofibers had a similar water uptake, but greater amount of bound water than the membrane without nanofibers. Although the proton conductivities in the perpendicular direction to the aligned fiber direction of the composite membranes were similar to that of the membrane without nanofibers, the proton conductivities in the parallel direction were higher than that of the membrane without

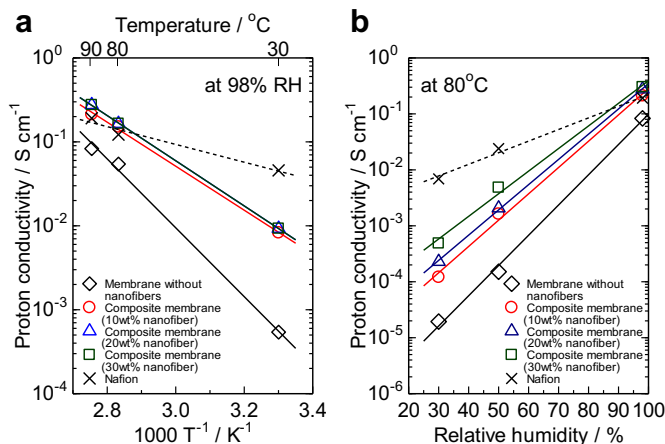


Fig. 5. (a) Temperature dependence (98% RH) and (b) relative humidity dependence (80 °C) on proton conductivity of the composite membranes, the membrane without nanofibers, and Nafion.

nanofibers and increased with the decreasing nanofiber diameters. The composite membranes containing thinner nanofibers and higher nanofiber contents showed an excellent parallel proton conductivity up to 0.3 S cm^{-1} at 90°C and 98% RH. It is considered that the ionic channels were formed in the nanofibers and that the protons were rapidly and efficiently transported in the nanofibers to enhance the conductivity. In addition, the chemical stabilities of the composite membranes were better than that of the membrane without nanofibers. Although the proton conductivities and membrane stabilities of the novel composite membranes are still insufficient for practical use in fuel cell applications, the new approach using nanofibers will promise future applications in fuel cells.

Acknowledgment

This work was partially supported by a grant from the Tokyo Metropolitan University, Japan and an ALCA grant from JST, Japan.

References

- [1] W. Vielstich, Handbook of Fuel Cells, Wiley, Chichester, England, 2009.
- [2] H.P. Dhar, J. Electroanal. Chem. 357 (1993) 237.
- [3] B.C.H. Steele, A. Heinzel, Nature 414 (2001) 345.
- [4] M.W. Verbrugge, R.F. Hill, J. Electrochem. Soc. 137 (1990) 3770–3777.
- [5] K.S. Rohr, Q. Chen, Nat. Mater. 7 (2008) 75–83.
- [6] J. Fang, X. Guo, S. Harada, T. Watari, K. Tanaka, K. Kita, K. Okamoto, Macromolecules 35 (2002) 9022–9028.
- [7] Y. Chikashige, K. Miyatake, M. Watanabe, Macromolecules 36 (2003) 9691–9693.
- [8] T. Nakano, S. Nagaoka, H. Kawakami, Polym. Adv. Technol. 16 (2005) 753–757.
- [9] J. Jouanneau, R. Mercier, L. Gonon, G. Gebel, Macromolecules 40 (2007) 983–990.
- [10] M.J. Park, K.H. Downing, A. Jackson, E.D. Gomez, A.M. Minor, D. Cookson, A.Z. Weber, N.P. Balsara, Nano Lett. 7 (2007) 3547–3552.
- [11] Y. Okazaki, S. Nagaoka, H. Kawakami, J. Polym. Sci. Part B Polym. Phys. 45 (2007) 1325.
- [12] K. Goto, I. Rozhanskii, Y. Yamakawa, T. Otsuki, Y. Naito, Polym. J. 41 (2008) 95–104.
- [13] T. Suda, K. Yamazaki, H. Kawakami, J. Power Sources 195 (2010) 4641–4646.
- [14] K. Yamazaki, H. Kawakami, Macromolecules 43 (2010) 7185–7191.
- [15] B.R. Einsla, Y.S. Kim, M.A. Hickner, Y.T. Hong, M.L. Hill, B.S. Pivovar, J.E. McGrath, J. Membr. Sci. 255 (2005) 141–148.
- [16] J. Pang, H. Zhang, X. Li, Z. Jiang, Macromolecules 40 (2007) 9435–9439.
- [17] C. Drew, X. Liu, D. Ziegler, X. Wang, F.F. Bruno, J. Whitten, L.A. Samuelson, J. Kumar, Nano Lett. 3 (2003) 143–147.
- [18] H. Jiaxing, R.B. Kaner, Nat. Mater. 3 (2004) 783–786.
- [19] Y. Dzenis, Science 305 (2004) 1917–1919.
- [20] A.C. Patel, S. Li, J.M. Yuan, Y. Wei, Nano Lett. 6 (2006) 1042–1046.
- [21] E. Formo, E. Lee, D. Campbell, Y. Xia, Nano Lett. 8 (2008) 668–672.
- [22] Y. Karube, H. Kawakami, Polym. Adv. Technol. 21 (2010) 861–866.
- [23] S. Fukushima, Y. Karube, H. Kawakami, Polym. J. 42 (2010) 514–518.
- [24] H. Na, X. Li, X. Hao, D. Xu, D. Zhang, S. Zhong, D. Wang, J. Membr. Sci. 281 (2006) 1–6.
- [25] Y.A. Elabd, J.D. Snyder, H. Chen, Macromolecules 41 (2008) 128–135.
- [26] R. Wycisk, P.N. Pintauro, P.T. Mather, J. Choi, K.M. Lee, Macromolecules 41 (2008) 4569–4572.
- [27] R. Takemori, H. Kawakami, J. Power Sources 195 (2010) 5957–5961.
- [28] T. Tamura, H. Kawakami, Nano Lett. 10 (2010) 1324–1328.
- [29] W. Jang, C. Lee, S. Sundar, Y.G. Shul, H. Han, Polym. Degrad. Stab. 90 (2005) 431–440.
- [30] K. Yamazaki, Y. Tang, H. Kawakami, J. Membr. Sci. 362 (2010) 234–240.